Author version: Geo-Mar. Lett.: 29(1); 2009; 25-38

Multidisciplinary investigations exploring indicators of gas hydrate occurrence in the Krishna–Godavari Basin offshore, east coast of India

M. V. Ramana*, T. Ramprasad, A. L. Paropkari, D. V. Borole, B. Ramalingeswara Rao, S. M. Karisiddaiah, M. Desa, M. Kocherla, H. M. Joao, P. Lokabharati, Maria-Judith Gonsalves, J. N. Pattan, N. H. Khadge, C. Prakash Babu,
National Institute of Oceanography, Dona Paula, Goa 403004, India
A. V. Sathe,
KDMIPE, Oil and Natural Gas Corporation Ltd., Dehradun 248195, India
P. Kumar,
IEOT, Oil and Natural Gas Corporation Ltd., Panvel, Mumbai 410221, India
and
A. K. Sethi
Directorate General of Hydrocarbons, New Delhi 110001, India

* Corresponding author: ramana@nio.org

Abstract

We report some main results of multidisciplinary investigations carried out within the framework of the Indian National Gas Hydrate Program in 2002–2003 in the Krishna–Godavari Basin offshore sector, east coast of India, to explore indicators of likely gas hydrate occurrence suggested by preliminary multi-channel seismic reflection data and estimates of gas hydrate stability zone thickness. Swath bathymetry data reveal new evidence of three distinct geomorphic units representing (1) a delta front incised by several narrow valleys and mass flows, (2) a deep fan in the east and (3) a WNW–ESE-trending sedimentary ridge in the south. Deep-tow digital side-scan sonar, multi-frequency chirp sonar, and sub-bottom profiler records indicate several surface and subsurface gas-escape features with a highly resolved stratification within the upper 50 m sedimentary strata. Multi-channel seismic reflection data show the presence of bottom simulating reflections of continuous to discrete character. Textural analyses of 76 gravity cores indicate that the sediments are mostly silty clay. Geochemical analyses reveal decreasing downcore pore water sulphate (SO_4^{2-}) concentrations (28.7 to <4 mM), increasing downcore methane (CH_4) concentrations (0–20 nM) and relatively high total organic carbon contents (1–2.5%), and microbial analyses a high abundance of microbes in top core sediments and a low abundance of sulphate-reducing bacteria in bottom core sediments. Methane-derived authigenic carbonates were identified in some cores. Combined with evidence of gasescape features in association with bottom simulating reflections, the findings strongly suggest that the physicochemical conditions prevailing in the study area are highly conducive to methane generation and gas hydrate occurrence. Deep drilling from aboard the *JOIDES Resolution* during 2006 has indeed confirmed the presence of gas hydrate in the Krishna–Godavari Basin offshore.

Introduction

Gas hydrate, or clathrate, is a crystalline molecular complex formed from mixtures of water and suitably sized gas molecules. Water crystallizes in the cubic crystallographic system, and forms a cage-like structure around a smaller ‘guest molecule’ such as methane, ethane, propane, isobutene, normal butane, nitrogen, carbon dioxide and hydrogen sulphide, of which methane is the most common (Kvenvolden 1993; Sloan 2000). Gas hydrate has received global attention as a possible alternative non-conventional energy resource. Several publications have described the significance, occurrence and formation/genesis of these valuable deposits both in permafrost regions and in marine sediments of continental slopes (e.g. Kvenvolden 1993; Holbrook et al. 1996; Sloan 1997; Ginsburg and Soloviev 1998; Collett et al. 1999; Collett and Ladd 2000; Milkov and Sassen 2001; Collett 2002).

The National Institute of Oceanography (NIO) of India has drawn up detailed maps of the thickness of the gas hydrate stability zone (GHSZ) in the Bay of Bengal, east coast of India (NIO 1997), using the Miles (1995) concept. The GHSZ map thereby generated predicts the presence of gas hydrate-bearing strata in the Krishna–Godavari, Bengal, Mahanadi and Cauvery offshore sectors (Fig. 1a). Exploration for conventional hydrocarbons is an ongoing activity since the last two decades in the Krishna–Godavari (KG) offshore, and drilling has confirmed the presence of huge gas deposits (Biswas 1999; Rao 2001). Indeed, some of the major oilfields—for example, in the Gulf of Mexico, the Norwegian Sea, and along the northern Cascadian margin— are long known not only for their conventional hydrocarbon potential but also for their gas hydrate accumulation fields (e.g. Brooks et al. 1986; Kennicutt et al. 1988; Bouriak et al. 2000; Riedel et al. 2001). Thus, the KG offshore, with its proven hydrocarbon potential, may also be a promising area for gas hydrate accumulation.

Preliminary examination of multi-channel seismic reflection profiles acquired by the Indian oil industry (Oil and Natural Gas Corporation Ltd., ONGC, and Reliance India Ltd., RIL) has revealed the presence of anomalous seismic reflections at depths below the seabed corresponding approximately with the base of the inferred GHSZ. These satisfy the criteria of typical bottom simulating reflections (BSRs; Dillon et al. 1994), implying the likely occurrence of gas hydrate deposits.

Within this context, we undertook a multidisciplinary study of geophysical and non-geophysical (geological, geochemical and microbial) datasets archived at NIO, India with the aim of

identifying a more powerful suite of proxy indicators that could serve to infer the occurrence of gas hydrates in the Krishna–Godavari offshore sector of the Bay of Bengal.

Geological setting

The eastern continental margin of India has evolved as a consequence of rifting and subsequent drifting from the contiguous Antarctica–Australia (Ramana et al. 2001). The KG Basin, located along the central east coast of India, occupies an onshore area of about 28,000 km^2 and extends beyond the mid-slope, encompassing an area of 1,45,000 km^2. The deepest basement rocks in the KG onshore basin are of Archean/Precambrian age, and the structural architecture is characterized by NE–SW-trending horsts and grabens filled with variable thicknesses of volcanic lava flows with intertrappen clay, limestone and sand beds of Upper Cretaceous to Recent age (Rao and Mani 1993; Rao 2001; Sahu 2005). Abnormal pressures due to advection of gases are observed especially in the Palaeogene deposits, these being the prospecting zones in the KG Basin (Rao and Mani 1993).

The KG offshore comprises predominantly claystone with minor sand and siltstone bands. The clay/claystone is grey to dark grey, soft and clastic with shell fragments and foraminifers. The thickness of this formation varies between 2,110 and 2,750 m, and is well developed in the Godavari offshore sector. The other geological formations comprise the Ragavapuram/ Vemavaram/ Chintalpalli/ Vadaparru shales over the Pre-Albian formation, while the Godavari clays of considerable thickness overlie the Vadaparru shale formation (Venkatarengan et al. 1993). To date, most discoveries of hydrocarbons in the KG offshore have been within sands deposited by turbidity flows (Raiverman et al. 1984; Sahu 2005). The Pliocene sandstone reservoir contains evidence of major Neogene growth faults related to the petroleum system in the upper slope region at 260–460 m water depths (Biswas 1999; Sahu 2005).

The hard collision between the Indian and Eurasian plates resulted in the building of the Himalayas (Curray et al. 1982). Subsequent monsoon activity promoted the rejuvenation of major rivers (Ganges, Brahmaputra, Mahanadi, Krishna, Godavari and Cauvery) and minor tributaries transporting huge amounts of sediments into the Bay of Bengal (Curray and Moore 1971). This sediment flow is manifested in the form of deltas and delta fronts. The Mahanadi, Krishna–Godavari and Cauvery offshore regions mark the delta fronts on the inner shelf, extending beyond the shelf break. The shelf is incised by headward-eroding point-source canyons which are now abandoned and filled with clay and reworked sediments. Several V-

shaped canyons flanked by steep faults characterize the upper to middle slope regions, while turbidity channels and levee wedges traverse the shelf and slope (Prasad and Rangaraju 1987). The high terrestrial input is a rich source of organic carbon, and its quick burial can result in methane generation.

Materials and methods

Three multidisciplinary cruises onboard the research vessels *ORV Sagar Kanya* and *AA Sidorenko* were undertaken during 2002–2003 to acquire geophysical, geological, geochemical and microbial data in the Krishna–Godavari Basin offshore sector. This was within the framework of the Indian National Gas Hydrate Program (NGHP) initiated by the Ministry of Petroleum and Natural Gas (MoP&NG), Government of India, and coordinated by the Director General of the Directorate General of Hydrocarbons (DGH, a wing of MoP&NG). Table 1 provides an overview of the instruments used and data types acquired, as well as of the selected datasets shown in the present study. Positioning was by means of a global positioning system (GPS and DGPS).

Geophysical data

A Hydrosweep system (M/s Atlas Elektronik GmBH, Germany) was used to acquire multibeam swath bathymetry data, the sound velocities computed from CTD observations (cf. below) being fed to the system. The data were processed by means of the public domain software MB System 4.6.10 (Caress and Chayes 1996), and a seafloor mosaic generated. All maps presented in this paper were generated using the GMT software of Wessel and Smith (1998).

We deployed a Geo Acoustics Deep Tow 2000 model (Geo Acoustics, UK), enabling simultaneous operation of a Chirp II profiler, side-scan sonar, magnetometer, responder and attitude sensor for obtaining seafloor images and highresolution subsurface information. These sensors are housed in a deep-tow body model 136 rated for 3,000 m water depth, connected to the recording system through a single coaxial tow cable. The data were acquired at a line spacing of 1 km (Fig. 1b). The side-scan sonar (114 kHz/410 kHz) and chirp sonar (500 Hz to 12 kHz) data were processed using the Geo-Pro 4 software within the system while acquiring the data. Post-processing was carried out to generate selected images of the seabed.

The processed multi-channel seismic sections used in the present study were provided by the Indian oil industry (cf.above; energy source 1,382 in.^{3}, shot interval 25 m, recording unit DFS V, sampling interval 2 ms, streamer length 3,000 m, and dominant frequency 50 Hz).

Geological data

A gravity corer (3.5 **t** head weight) was used to collect 5–6 m long sediment cores at 76 sites (Fig. 1c). Grain-size determination was by means of a laser particle size analyzer. Physical properties, namely water content, specific gravity, porosity and wet bulk density, were determined based on methods proposed by Raj (1995) and Das (1998).

Geochemical data

Pore waters were extracted from the cores, and analysed for SO_4^{2-} and Cl^- at 50-cm intervals. A Dionex ion chromatograph DX-600 served for the determination of sulphate (cf. Gieskes et al. 1991), whereas Cl^- was measured using the Mohr titration procedure (Grasshoff et al. 1983).

Free and adsorbed gases were extracted from wet sediment subsamples at three core levels, i.e. top, middle and bottom, using a vacuum sediment degassing system (Schmitt et al. 1991). Methane was determined with a Carlo Erba model CE-8000 TOP gas chromatograph, using 30-mlong GS-Q coated quartz capillary column and flame ionization detector.

Calcium carbonate was estimated in subsamples by the weight loss method, and total organic carbon (TOC) by titrimetry.

Microbial data

Seeing that, in gas hydrate-bearing sediments, bacterial degradation of organic matter is achieved by a complex consortium of bacteria and microbes (e.g. Whiticar 1999; Borowski et al. 1999), aliquots of core material were analyzed at three core depths, i.e. surface, middle and bottom, for four key groups: (1) fermenters, (2) sulphatereducing bacteria, (3) nitrate-reducing bacteria and (4) nitrifying bacteria. The sulphate-reducing bacteria were enumerated using Hatchikian's medium prepared in seawater (Hatchikian 1972; Loka Bharathi and Chandramohan 1985). Fermenters grew in sulphate-reducing bacteria medium but without precipitation of sulphide utilizing acetate and lactate. Nitrate-reducing and nitrifying bacteria were estimated using the methodology of Rodina (1972).

CTD data

A CTD system (SBE911 plus, M/S Seabird Electronics Ltd., USA) was used to generate vertical profiles of water temperature, salinity, and dissolved oxygen at 11 sites (Fig. 1c).

Results

Geophysical characteristics

Swath bathymetry and high-resolution shallow seismics

The study area (Fig. 1) covers the upper to mid slope region of the eastern continental margin of India, and the depth to the seabed varies from <400 m near the coast to >2,000 m offshore. The swath bathymetry mosaic depicts (1) a toe-like delta front at water depths of <400–600 m in the north, extending up to 16°04′ N between 81°54′ and 82°10′ E, (2) a fan-like geomorphic unit, with a gradual increase in water depths from 1,200 to >1,900 m, extending in a southeasterly direction between 82°14′ and 82°30′ E and (3) an approximately WNW–ESE-trending sedimentary ridge in the south-western part of the study area (Fig. 2).

The fan-like system observed in the eastern part of the study area is bounded by an approx. E–W- and NNW–SSE-trending scarp/steep fault-like structural elements in the north and west, respectively. It is characterized by a smooth topography with a gentle gradient deepening offshore.

The seafloor is relatively rugged between the NNW–SSE-trending fault and the WNW–ESE-trending sedimentary ridge, with a few positive bathymetric features around 82°06′ E. There are several mudflows due to slumping/sliding, which disappear in the vicinity of the inferred toe thrust fault at approx. 1,600 m depth. The delta front is incised with several valleys. The effect of slumping/sliding is seen in the mid-slope region in the form of sediment flows and sediment buildup (Fig. 2). The sedimentary ridge, with an overall basal width of about 10 km, rises to <950 m above the seafloor at a water depth of 1,400 m. West of this ridge, there are linear turbidity channels bounded by steep scarps.

The deep-tow digital side-scan, chirp sonar and subbottom profiler datasets acquired along the cruise tracks (Fig. 1b) over the BSR-prone area depict complex surface and subsurface features. Side-scan sonar images show swarms of pockmarks (30–40 m diameter), and the corresponding chirp sonar records show evidence of surface and subsurface disturbance (Fig.

3). Gas-escape features such as gas chimneys, zones of gas masking/saturation, and mud diapirs are common (Fig. 4). Acoustic pipes and gas chimney/mud diapir-like features are seen cutting the sedimentary layers (Fig. 4a). The presence of a strong reflector at around 25 m below the seabed indicates the likely occurrence of gas masking/saturated sediments below it. The pockmark in Fig. 4b may be due to gas/fluid expulsion. The discontinuous nature of the strong reflector below the pockmark indicates gas saturation.

There is evidence of faulting in the subsurface layers, with a throw of about 5–20 m. A fault-controlled mud diapir-like feature is inferred in Fig. 4c. The gas accumulation associated with the diapir has also affected the seafloor and subsurface horizons. Slumping is seen along line S2, and the subsurface sediments are oversaturated with gas, as indicated by the presence of pockmarks and an irregular reflection-free topography (Fig. 4d). The chirp sonar records also depict a sub-bottom penetration of >50 m below the seabed, with high-resolution stratification. The sub-bottom profiler records (Fig. 5) show the presence of pockmarks and mud diapirs about 20–100 m high.

Multi-channel seismics and BSRs

BSRs in general can be inferred by (1) mimicking of the seafloor topography with polarity reversal, (2) crosscutting of lithological boundaries and (3) amplitude blanking above and below anomalous reflections. In the present study, this is reported for three multi-channel seismic sections, AD-94- 11 and AD-94-17 (dip lines) and GDSW-46 (strike line; cf. Fig. 1b). The data show BSRs occurring at around 200–320 ms below the seafloor (Figs. 6 and 7), mostly continuous to discrete in character.

Line AD-94-11 lies on the northern flank of the sedimentary ridge (Fig. 6). A low-relief anticline structure occurs below the BSR, and this horizon is characterized by several faults. The upper strata above the BSR are devoid of continuous reflections, suggesting that the sediment pore space could contain gas hydrate, or that the sediments are of homogeneous clay/silty clay. Draping of sediments on the seabed is attributed to sliding (between shots 225 and 250). The disturbed nature of the BSR is observed immediately below a slump-like feature on the seabed, between shots 338 and 350.

The BSR along line AD-94-17 crosscuts the lithology towards the southeast (Fig. 7). Towards the northwest, the BSR is continuous between shots 189 and 269. Several subsurface geological horizons associated with faults are common in this region. There is evidence of a

typical buried carbonate reef between shots 100 and 190. A distinct basin-like feature occurs, with onlap of younger sediments between shots 150 and 480. Towards its northwest, a domelike feature associated with faults is seen in the subsurface layers between shots 30 and 150. There is evidence of slumping on the seabed between shots 100 and 120.

The BSR along line GDSW-46 is distinct towards the southwest and discrete, merging with the subsurface lithology in the northeast (Fig. 8). This section shows evidence of several faults and gas-related features. The anticline-like feature (shale bed) observed also on line AD-94-11 is more conspicuous here, with a relief of about 300 ms (~240 m). There is a mud diapir in the form of an intrusion towards the northeast. Deposition of recent sediments is seen towards the southwest.

Geological characteristics

All 76 gravity cores (5–6 m long) are characterized by loose sediments within the top 60 cm. The top 0–40 cm sediments are moderately yellowish brown, whereas the remaining core lengths are greyish olive with minor variations. The sediments contain very low amounts of coarse-grained material (<1% calcareous sand); silt content is ~23% and clay content 72–82%. KG offshore sediments can therefore be classified as silty clay, according to the scheme of Folk (1968). Downcore values of absolute water content, porosity and wet bulk density vary in the range 50–56%, 55–60% and 1.4–1.5 g/cm3, respectively. Specific gravity and specific surface area are 2.20–2.56 and 1.6–2.6 m2/g, respectively.

Geochemical characteristics

Pore water sulphate (SO_4^{2-}) concentrations vary markedly from 28 mM at the top of the gravity cores, to 4 mM at the bottom. At 48 of the 76 core locations, SO_4^{2-} concentrations show a particularly distinct decreasing trend with core depth. At two locations (stations 20 and 36, Fig. 1c), the values are as high as 33 mM in the top sediments and nearly zero at the core bottom. Pore water chloride (Cl^-) concentrations vary between 420 and 560 mM, and show no marked downcore trends.

Methane (CH_4) concentrations in the study area generally vary between 0.2 nM in the top sediments and 20 nM in the bottom sediments. However, at one location (GC07, Fig. 1c) south of the WNW–ESE-trending sedimentary ridge, CH_4 concentration is as high as 153 nM in the bottom sediments (Fig. 9). The sulphate–methane interface can be inferred below 5 m core

depth. This core also had a strong H_2S odour. Downcore enrichment of CH_4 is particularly evident at 23 of the 76 locations.

TOC contents in general are around 1% in the top sediments, and around 2% in the bottom sediments. At two locations (stations 46 and 62) in the mid-slope region (Fig. 1c), the TOC values are as high as 2.5% in the bottom sediments. Downcore $CaCO_3$ contents in general vary between 4% and 16%.

Microbial characteristics

In the gravity cores, nitrifying bacteria are abundant in the top sediments, varying between 6×103 and 1×104 cells per gram. By contrast, they are totally absent in the bottom core sediments. Sulphate-reducing bacteria (ca. 1.9×104 cells per gram) and fermenters (ca. 2.14×103 cells per gram) are also abundant at the surface but scanty (~1×102 cells per gram) in the bottom sediments, as are nitrate-reducing bacteria (1.2×104 and ~1×102 cells per gram in the top and bottom core sediments, respectively).

CTD characteristics

The CTD measurements of winter (December) 2002 indicate a sea surface temperature of 26.0°C for the study area. Near-bottom temperatures varied from 10.5 to 5.0°C between ~400 and 1,600 m water depths. Surface salinity was 27.0–29.0 psu.

Dissolved oxygen (DO) concentration was about 4.5 ml/l at the sea surface, decreasing sharply to 0.4 ml/l between 100 and 600 m water depths. DO then increased again to 1.5–1.8 ml/l towards the sea bottom.

Discussion and conclusions

The swath bathymetry mosaic described above for the Krishna–Godavari Basin offshore shows the complex nature of the seabed in the form of a delta front, a fault controlled fan-like system, and a WNW–ESE-trending sedimentary ridge. The delta front between the outer shelf and upper slope, i.e. between <400 and 600 m water depths, in the north of the study area is incised with valleys/canyon-like features and scarps caused by turbidity flows, and evolved during the late Miocene to Holocene (Prasadand Rangaraju 1987). The smooth topography of the fan suggests that the faults are controlling the debris flow from the adjacent areas. The proximal end seems to be serving as inlet for sediment flow into the fan.

The WNW–ESE-trending sedimentary ridge is a major geomorphic feature with a gentle northward gradient reflecting slow accumulation of sediment, whereas the relatively steep gradient towards the south suggests negligible deposition of sediments. This ridge may be acting as a barrier for terrestrial input, and serving as a structural trap for gas accumulation. The observed highly irregular topography, associated with scars, slides, slumps and other deformation features, can be explained by massive clastic input from the Krishna–Godavari delta, passing directly onto the extensive and coeval slope and into the deepwater sedimentary system, as suggested by Sahu (2005).

The present study has demonstrated the occurrence of gas-escape features such as pockmarks, mud diapirs, gas vents/chimneys/pipes, gas masking/saturation and blanking. Most hydrocarbon fields and gas hydrate-prone areas occurring in various world regions are associated with gas-escape features (e.g. Hovland and Judd 1988; Milkov 2004). The offshore sector of the Krishna–Godavari Basin has been known for its hydrocarbon potential as well as the presence of BSRs since the earlier studies of Rao (2001), Sahu (2005) and Ramana et al. (2006). These findings suggest this area is also a potential gas hydrate province. Most of the observed gas-escape features can be explained by the vertical migration of subsurface gas/fluid expulsion caused by excessive in situ pressures. Such pressures may be due to gas saturation, which has also disturbed the subsurface layers. These gas-escape features can be considered as primary proxies for gas hydrate occurrence in marine sediments of the Krishna–Godavari offshore sector.

The processed multi-channel seismic sections showing continuous to discrete BSRs in the present study also reveal that the strata above and below these BSRs are associated with faults of different magnitudes, some of which may be serving as conduits for gas/fluid migration. These faults can be explained by tectonic disturbances caused either by sediment slope failure/instability or by neotectonic activity. Murthy et al. (1993, 1995) reported the presence of neotectonic activity in the study area. The long-wavelength low-relief subsurface swell/anticline in the vicinity of the inferred WNW–ESE-trending sedimentary ridge is due to the effect of shale diapirism (Sahu 2005). The inferred basin and shale diapirism can be explained by extensional and compressional regimes, respectively, in the KG Basin offshore sector, whereby the shale diapirism has uplifted the strata above. The similarity of the crest observed on the seafloor and the shale diapir, and the undisturbed nature of the sedimentary sequence in between indicate that upliftment might have occurred in recent times. Oversaturation and expulsion of gas/fluid in combination with these compressional forces could explain the formation of mud diapirs.

The steep gradient (~1:32) of the seafloor and the high terrestrial input due to intense Indian monsoons might be the forces responsible for the observed slumping/slides in the study area. The occurrence of high-volume sediment slope failures between 13,000 and 11,000–8,000 years B.P. has been correlated with rising sea levels, and peaks in atmospheric methane levels due to disintegration of gas hydrates in the North Atlantic sector, including the Nordic seas and the Mediterranean Sea (Maslin et al. 2004). Similar slide scarps have been reported in offshore regions of Norway (Brown et al. 2006). Therefore, we suggest that sea-level fluctuations can be considered as an alternative explanation for the slumping/slides observed in the present study.

The finding that the sediments in the study area are mostly silty clay with negligible sand fractions is consistent with the inferences of Rao (2001), who identified the Quaternary-Holocene alluvial cover on land as Andhra alluvium, and the offshore clay sequence overlying the Ravva formation (Miocene–Pliocene–Pleistocene) as Godavari clays. Independent evidence exists that these fine sediments are not confined to the top 5 m but continue several hundred meters deep below the seabed (Pandey and Dave 1998). Furthermore, sedimentological analyses of cores collected during the NGHP Expedition 01 exploring for gas hydrates along the KG Basin offshore show the presence of thin lenses of sand in silty clay and claydominated fractured reservoirs (Collett et al. 2007). The Ocean Drilling Program (ODP) results for, e.g. the Blake Ridge area and the Cascadian Margin, eastern and western margins of America, respectively, and the Nankai Trough off Japan, reveal that organic-rich clays are also favourable hosts for gas hydrate deposits (Lorenson and Collett 2000; Milkov et al. 2004).

Martens and Klump (1984) and Borowski et al. (1999) suggested that regions with large inputs of organic matter are prone to high methane production. The rate of sedimentation in the KG offshore sector is about 40 cm/1,000 years (Sarin et al. 1979; KDMIPE, ONGC, Dehradun, personal communication). Such rapid sedimentation would facilitate the preservation of buried organic carbon in the sediments, and its fermentation would result in insitu generation of methane. This is consistent with the increasing downcore TOC enrichment (ca. 1% in top sediments, versus >2.0% in bottom sediments), and the reverse pore water SO_4^{2-} trend recorded in the present study.

Microbial activity depletes pore water sulphate with increasing sediment depth and, at the base of this sulphate reduction zone, methane and sulphate are totally consumed by anaerobic methane oxidation (Reeburg 1976; Borowski et al. 1999). The marked downcore decrease in pore water SO_4^{2-} (from 28 to ~4 mM) recorded in the study area indicates the onset of anoxic

conditions at depth, where sulphate and methane have been co-consumed by microbes. An example of such distinct geochemical characteristics is seen at location GC07 in the study area. Examples from other regions include the Blake Ridge (Lorenson and Leg164 Shipboard Scientific Party 2000), and the Cascadian margin (ODP Leg 146 Shipboard Scientific Party 1994). The downcore decrease in sulphate- and nitrate-reducing microbial populations documented in the present study is another indication of anoxic conditions in deeper sediments, extending to the base of the sulphate minimum (sulphate–methane interface).

At first glance, methane concentrations in the present study would seem comparatively low, generally not exceeding about 20 nM. For example, much higher values of about 1,786 nM have been reported off Pakistan (Von Rad et al. 1996). In the present case, however, we attribute these low values at least partly to the slow recovery speed at which core samples were collected from the seabed. Evidently, this aspect would deserve closer attention in future studies attempting to collect long cores and extract methane gas for exploration purposes in the Krishna–Godavari Basin.

Hardage and Roberts (2006) have summarized the mechanism of hydrate formation in the Gulf of Mexico by adopting the concept of Borowski et al. (1999) which states that, on reaction with dissolved sulphate at the seafloor, free methane forms carbonates (HCO_3) along with H_2S and water. Evidence of pockmarks and other gas-escape features, as well as faults and buried carbonate reefs in the present study area suggests an upward flow of in situ methane possibly associated with the formation of carbonates. Moreover, some of the cores were characterized by a strong H_2S odour. Indeed, based on tonal variations in deep-tow digital side-scan sonar images, the presence of carbonate mats has been inferred on the seabed (NIO 2005). Furthermore, carbonate fragments have been identified at various depths of some sediment cores used in the present study (Kocherla et al. 2006) and, using detailed XRD, SEM, and $\delta^{13}C$ isotopic analyses, these have been interpreted as being primarily methane-derived.

The geophysical, geological, geochemical and microbial parameters assessed in this multidisciplinary investigation are therefore considered as powerful proxy indicators for predicting gas hydrate occurrence in the KG offshore sector and, for that matter, in other promising offshore exploration areas in the Bay of Bengal. Our findings would predict that regions around and towards the north of the WNW–ESE trending sedimentary ridge are the most promising for detailed gas hydrate exploration. Indeed, recent drilling from onboard the research vessel JOIDES Resolution in 2006 has confirmed the presence of gas hydrate in the

study area. At one location (Fig. 1b), a massive hydrate of 130 m thickness (Fig. 10) has been recovered at a water depth of approx. 1,038 m. Moreover, most of the drill sites are associated with gas hydrate chunks or 30–40% gas saturation in pore spaces (Collett et al. 2007).

The abundance of gas-escape features observed within the shallow sedimentary strata of the KG Basin offshore sector raises the possibility that methane gas may be from dissociated gas hydrate, in addition to methane generated in situ. Future assessments of much deeper cores, and the acquisition of additional high-resolution multi-channel seismic reflection data would greatly improve our understanding of the geochemical environment, and the spatial and temporal distribution patterns of gas hydrate accumulations in the Krishna–Godavari Basin offshore, the east coast of India, and other promising exploration sites along the Indian continental margins.

Acknowledgements We acknowledge the Director, NIO, Goa, for granting necessary permission to publish this article. We sincerely thank Prof. K. Andreassen, University of Tromsø, and Dr. R. Bøe, Geological Survey of Norway, for their critical reviews, and Drs. T. Lorenson, USGS, California, and M.T. Delafontaine, journal editor, for useful suggestions. We are indebted to Mr. V.K. Sibal, Director General of Directorate General of Hydrocarbons, for his constant encouragement. The crew and officers of the *ORV Sagar Kanya* and *AA Sidorenko*, scientific and technical staff from NIO are acknowledged for their cooperation during data acquisition. This is NIO contribution no. 4388.

References

Biswas AK (1999) Hydrocarbon exploration perspectives of frontier basins of India. In: Bhatnagar AK et al (ed) Hydrocarbon exploration. Papers in the 3rd International Petroleum Conference and Exhibition, PETROTECH-99, vol. 4. Thomson, Haryana, pp 31–39

Borowski WS, Paull CK, Ussler W (1999) Global and local variations of interstitial sulfate gradients in deep-water, continental margin sediments: sensitivity to underlying methane and gas hydrate. Mar Geol 159:131–154

Bouriak S, Vanneste M, Saoutkien A (2000) Inferred gas hydrates and clay diapirs near the Storegga slide on the southern edge of the Oring Plateau, offshore Norway. Mar Geol 163:125–148

Brooks JM, Cox HB, Bryant WR, Kennicutt MC, Mann RG, McDonald TJ (1986) Association of gas hydrates and oil seepage in the Gulf of Mexico. Org Geochem 10:221–234

Brown HE, Holbrook WS, Hornbach MJ, Nealon J (2006) Slide structure and role of gas hydrate at the northern boundary of Storegga slide, offshore Norway. Mar Geol 3/4:179–186

Caress DW, Chayes DN (1996) Improved processing of Hydrosweep DS multibeam data on the R/V Maurice Ewing. Mar Geophys Res 18:631–650

Collett TS (2002) Energy resource potential of natural gas hydrate. AAPG Bull 86(11):1971–1992

Collett TS, Ladd J (2000) Detection of gas hydrate with downhole logs and assessment of gas hydrate concentrations (saturations) and gas volumes on the Blake Ridge with electrical resistivity log data. In: Paull CK, Matsumoto R, Wallace PJ, Dillon WP (eds) Proceedings of the ODP, Science Results, vol 164, pp 179–191

Collett TS, Lewis RE, Dallimore SR, Lee MW, Mroz TH, Uchida T (1999) Detailed evaluation of gas hydrate reservoir properties using JAPEX/JNOC//GSC Mallik 2L-38 gas hydrate research well downhole well-log displays. In: Dallimore SR, Uchida T,Collett TS (eds) Scientific results from JAPEX/JNOC//GSC Mallik 2L-38 gas hydrate research well, Mackenzie delta, North-west Territories, Canada. Geological Survey of Canada Bulletin, Canada

Collett TS, Riedel M, Cochran JR, Boswell R, Presley J, Kumar P, Sathe A, Sethi A, Lall M, Sibal V, NGHP Expedition 01 Scientists (2007) National Gas Hydrate Program Expedition 01 initial reports. Directorate General of Hydrocarbons, New Delhi

Curray JR, Moore DG (1971) Growth of Bengal deep sea fan and denudation in the Himalayas. Geol Soc Am Bull 82:563–572 Curray JR, Emmel FJ, Moore DG, Raitt RW (1982) Structure, tectonics and geological history of the Northeastern Indian Ocean. In: Nairn AE, Stehli FG (eds) The ocean basins and margins, vol. 6. Plenum, New York, pp 399–450

Das BM (1998) Principles of geotechnical engineering. PWS, Boston, MA

Dillon WP, Lee MW, Coleman DF (1994) Identification of marine hydrates in situ and their distribution off the Atlantic coast of the United States. In: Proceedings of the International Conference of Natural Gas Hydrates, Annals of the New York Academy of Sciences, no 715, pp 364–380

Folk RL (1968) Petrology of sedimentary rocks. Hemphill, Austin, TX Gieskes JM, Gamo T, Brumsack H (1991) Chemical methods for interstitial water analysis aboard JOIDES Resolution. ODP technical note 15. Ocean Drilling Program, Texas A&M University, College Station, TX

Ginsburg GD, Soloviev VA (1998) Submarine gas hydrate. VNIIOkeangeologia, Saint Petersburg Grasshoff K, Ehrhardt M, Kremling K (1983) Methods of seawater analysis. Verlag Chemie, Weinheim

Hardage BA, Roberts HH (2006) Gas hydrate in the Gulf of Mexico: what and where is the seismic target? Leading Edge 25(5):566– 571

Hatchikian EC (1972) Mécanismes d'oxido-réduction chez les bactéries sulfato-réductrices. Ph.D. Thesis, University of Marseilles, Marseilles

Holbrook WS, Hooskins H, Wood WT, Stephen RA, ODP Leg 164 Scientific Party (1996) Methane hydrate, bottom simulating reflectors, and gas bubbles: results of vertical seismic profiles on the Blake Ridge. Science 273:1840–1843

Hovland M, Judd AG (1988) Seafloor pockmarks and seepages: impact on geology, biology and the marine environment. Graham and Trotman, London

Kennicutt MC, Brooks JM, Denoux GJ (1988) Leakage of deep, reservoired petroleum to the near surface of the Gulf of Mexico continental slope. Mar Chem 24:39–59

Kocherla M, Mazumdar A, Karisiddaiah SM, Borole DV, Rao BR (2006) Evidences of methane-derived authigenic carbonates from the sediments of the Krishna–Godavari Basin, eastern continental margin of India. Curr Sci 91(3):318–323

Kvenvolden KA (1993) Gas hydrate—geological perspective and global change. Rev Geophys 31:173–187

Loka Bharathi PA, Chandramohan D (1985) Sulphate reducing potential in an estuarine beach. Ind J Mar Sci 14:187–191

Lorenson TD, Collett TS (2000) Gas content and composition of gas hydrate from sediments of the southeastern North American continental margin. In: Paull CK, Matsumoto R, Wallace PJ,

Dillon WP (eds) Proceedings of the ODP, Science Results, vol 164, pp 37–46

Lorenson TD, Leg 164 Shipboard Scientific Party (2000) Graphic summary of gas hydrate occurrence by proxy measurements across the Blake Ridge, Sites 994, 995, and 997. In: Paull CK,Matsumoto R, Wallace PJ, Dillon WP (eds) Proceedings of the ODP, Science Results, vol 164, pp 247–249

Martens CS, Klump JV (1984) Biogeochemical cycling in an organic rich coastal marine basin. 4. An organic carbon budget for sediments dominated by sulfate reduction and methanogenesis. Geochim Cosmochim Acta 48:1987–2004

Maslin M, Owen M, Day S, Long D (2004) Linking continental slope failures and climate change: testing the clathrate gun hypothesis. Geology 32:53–56

Miles PR (1995) Potential distribution of methane hydrate beneath the European continental margins. Geophys Res Lett 22:3179–3182

Milkov AV (2004) Global estimates of hydrate bound gas in marine sediments: how much is really out there? Earth Sci Rev 66:183–197

Milkov AV, Sassen R (2001) Estimate of gas hydrate resource, northwestern Gulf of Mexico continental slope. Mar Geol 179:71–83

Milkov AV, Claypool GE, Lee Y-J, Torres MR, Borowski WS, Tomaru H, Sassen R, Long PE, ODP Leg 204 Scientific Party (2004) Ethane enrichment and propane depletion in subsurface gases indicate gas hydrate occurrence in marine sediments at southern Hydrate Ridge offshore Oregon. Org Geochem 35:1067–1080

Murthy KSR, Rao TCS, Subrahmanyam AS, Malleswara Rao MM, Lakshminarayana S (1993) Structural lineaments from magnetic anomalies of eastern continental margin of India (ECMI) and northwest Bengal Fan. Mar Geol 114:171–183

Murthy KSR, Subrahmanyam AS, Lakshminarayana S, Chandrasekhar DV, Rao TCS (1995) Some geodynamic aspects of the Krishna–Godavari Basin, east coast of India. Cont Shelf Res 15:779–788

NIO (1997) Gas hydrate resource map of India no. NIO/SP-25/97. National Institute of Oceanography, Dona Paula, Goa NIO (2005) Geoscientific investigations of shallow sediments in KG offshore, East Coast. Rep no NIO/TR-13/2003. National Institute of Oceanography, Dona Paula, Goa

ODP Leg 146 Shipboard Scientific Party (1994) Sites 892 and 889 [Leg 146]. In: Westbrook GK et al (eds) Proceedings of the ODP, Initial Report, vol 146, pp 301–396

Pandey J, Dave A (1998) Stratigraphy of Indian petroliferous basins. In: Proceedings of the XVI Indian Coll Micropaleontology and Stratigraphy. ONGC Ltd., Mumbai

Prasad KL, Rangaraju MK (1987) Modern and recent canyon-fan systems in Masulipatnam Bay, Krishna–Godavari Basin. Bull ONGC 24(2):59–71

Raiverman V, Rao MR, Pal D (1984) Stratigraphy and structure of Pranhita–Godavari Graben. Petrol Asia J 8(3):174–189

Raj P (1995) Geotechnical engineering. Tata-McGraw Hill, New Delhi

Ramana MV, Ramprasad T, Desa M (2001) Seafloor spreading magnetic anomalies in the Enderby Basin, East Antarctica. Earth Planet Sci Lett 191:241–255

Ramana MV, Ramprasad T, Desa M, Sathe AV, Sethi AK (2006) Gas hydrate-related proxies inferred from multidisciplinary investigations in the Indian offshore areas. Curr Sci 91(2):183–189

Rao GN (2001) Sedimentation, stratigraphy, and petroleum potential of Krishna–Godavari basin, east coast of India. AAPG Bull 85 (9):1623–1643

Rao GN, Mani KS (1993) A study on generation of abnormal pressures in Krishna Godavari Basin, India. Ind J Petrol Geol 2 (1):20–30

Reeburg WS (1976) Methane consumption in Cariaco trench waters and sediments. Earth Planet Sci Lett 28:337–344

Riedel M, Spence GD, Chapman NR, Hyndman RD (2001) Deep-sea gas hydrates on the northern Cascadia margin. Leading Edge 20 (1):87–91

Rodina AG (1972) Methods in studying microorganisms of the nitrogen cycle. In: Colwell RR, Zambruski MS (eds) Methods in aquatic microbiology. University Park Press, Baltimore, MD, pp 251–322

Sahu JN (2005) Deep water Krishna–Godavari basin and its potential. Petromin (Asia's Exploration and Production Business magazine), April issue, pp 26–34

Sarin MM, Borole DV, Krishnaswami S (1979) Geochemistry and geochronology of sediments from the Bay of Bengal and the equatorial Indian Ocean. Proc Ind Acad Sci 88:131–154

Schmitt M, Faber E, Botz R, Staffers P (1991) Extraction of methane from seawater using vacuum degassing. Anal Chem 63:529–531

Sethi AK, Ahmad MN (2006) Gas hydrates—a future energy source: advances in India, vol. 1(1). Petroview, Directorate General of Hydrocarbons, New Delhi, pp 5–10

Sloan ED Jr (1997) Clathrate hydrates of natural gases. Marcel Dekker, New York Sloan ED Jr (2000) Hydrate engineering. Monograph 21. SPE, Richardson, TX

Venkatarengan R, Rao GN, Prabhakar KN, Singh DN, Awasthi AK, Reddy PK, Mishra PK, Roy SK (1993) Lithostratigraphy of Indian petroliferous basins. Document VIII, Krishna–Godavari Basin. KDMIPE, ONGC, Dehradun

Von Rad U, Roesch H, Berner U, Geyh M, Marchig V, Schulz H (1996) Authigenic carbonates derived from oxidized methane vented from the Makran accretionary prism off Pakistan. Mar Geol 136:55–77

Wessel P, Smith WHF (1998) New improved version of Generic Mapping Tools released. EOS Trans AGU 79:579

Whiticar MJ (1999) Carbon and hydrogen isotope systematics of bacterial formation and oxidation of methane. Chem Geol161:291–314

Table 1

Instrument/data type	Total quantity	Selected datasets
Swath bathymetry	4,100 line km, coverage 3,400 km2 (Fig. 1b)	Figs. 1b, 2 (whole dataset)
CTD	11 stations (Fig. 1c)	Fig. 1c (whole dataset)
Side-scan sonar	1,100 line km (Fig. 1b)	Figs. 1b, 3
Digital chirp sonar	950 line km (Fig. 1b)	Figs. 1b, 3, 4
Sub-bottom profiler	1,100 line km (Fig. 1b)	Figs. 1b, 5
Gravity cores	76 stations (Fig. 1c)	Figs. 1c, 9
Multi-channel seismics	45 km (Fig. 1b)	Figs. 1b, 6, 7, 8

Table 1 Instruments used and data types acquired, as well as selected datasets reported in more detail in the present study

Fig. 1 a Map showing the thickness of the gas hydrate stability zone (GHSZ, in m) for the eastern continental margin of India (NIO 1997). Thin continuous lines Depth contours (m), dashed lines and thick lines oceanic fracture zones and magnetic anomaly lineations, respectively (Ramana et al. 2001), box study area in the Krishna–Godavari offshore sector. b Tracks along which deep-tow digital side-scan sonar, chirp sonar and sub-bottom profiler data (thin straight lines) were collected, superimposed on the bathymetry (contours in meters). Thick lines Multichannel seismic profiles reported in the present study, black star location of the JOIDES drill site, red lines selected datasets dealt with in more detail in the present study. c Locations of gravity cores (red dots) and CTD stations (black triangles), superimposed on the bathymetry (contours in meters). Black star Location of the JOIDES drill site, green square location of gravity core GC07

Fig. 2 a Detailed bathymetry of the study area (50-m contour interval). b Seafloor mosaic derived from swath bathymetry data. The major geomorphic features identified are a delta front (DF) with valleys and canyons, a toe thrust fault (TTF, dashed line), turbidity channels (TC), a sedimentary ridge (SR), a fan, slumps/slides (SL) and scars (SC). White patch at top Data gap resulting from this area being occupied by drilling rigs

Fig. 3 Deep-tow digital side-scan sonar and corresponding chirp sonar images along a line S9 and b line S7, showing a swarm of pockmarks and subsurface disturbance (cf. Fig. 1b for locations of the images)

Fig. 4 Chirp sonar records along a line S9, b line S7, c line S9 and d line S2, depicting the presence of gas-escape features such as gas chimneys (GC), mud diapirs (MD), pockmarks (PM), gas-saturated sediments/ acoustic masking (GSS) and gas/fluid expulsion in the form of acoustic pipes (G/F). Sub-bottom penetration is about 50 m below the seabed (SB). Solid lines Faults (cf. Fig. 1b for locations of the records)

Fig. 5 Sub-bottom profiler records showing mud diapirs (MD) and pockmarks (PM) along a line Cl2 and b line S14. Solid lines Faults (cf. Fig. 1b for locations of the records)

Fig. 6 Processed multi-channel seismic section along line AD-94-11, showing evidence of a fairly continuous BSR mimicking the seafloor, a low-relief anticline-like feature and subsurface strata associated with several faults (red), the imprint of a slide between shots 225 and 250, and a slump-like feature between shots 338 and 350, with its effect

in the form of a disturbed BSR. Data on the left Seabed with positive polarity, and BSR with negative polarity (cf. Fig. 1b for location of the section)

Fig. 7 Processed multi-channel seismic section along line AD-94-17, showing evidence of a faint BSR crosscutting the lithological units, extensive faulting (red), the imprint of a slump in the northwest, a basin-like feature filled with recent sediments, and a buried carbonate reef (CR). Data on the left Seabed with positive polarity, and BSR with negative polarity (cf. Fig. 1b for location of the section)

Fig. 8 Processed multi-channel seismic section along line GDSW-46, depicting a discrete BSR, merging with the subsurface lithology towards the NE. Deep drilling in its vicinity has revealed the presence of a thick gas hydrate column (Sethi and Ahmad 2006). The anticline-like feature (shale bed) identified also on line AD-94-11 is more conspicuous here. Towards the northeast, a mud diapir (MD) is seen in the form of an intrusion. The subsurface sedimentary strata between the seabed and the anticline-like feature are associated with faults (red) and gas-related features (cf. Fig. 1b for location of the section)

Fig. 9 Composite plot showing downcore variations in sulphate, methane and chloride concentrations in gravity core GC07 (cf. Fig. 1c for location). The sulphate–methane interface (SMI) can be inferred below 5 m core depth

Fig. 10 Photographs showing massive and disseminated gas hydrate samples recovered during NGHP Expedition 01 in the Krishna–Godavari offshore (Sethi and Ahmad 2006)

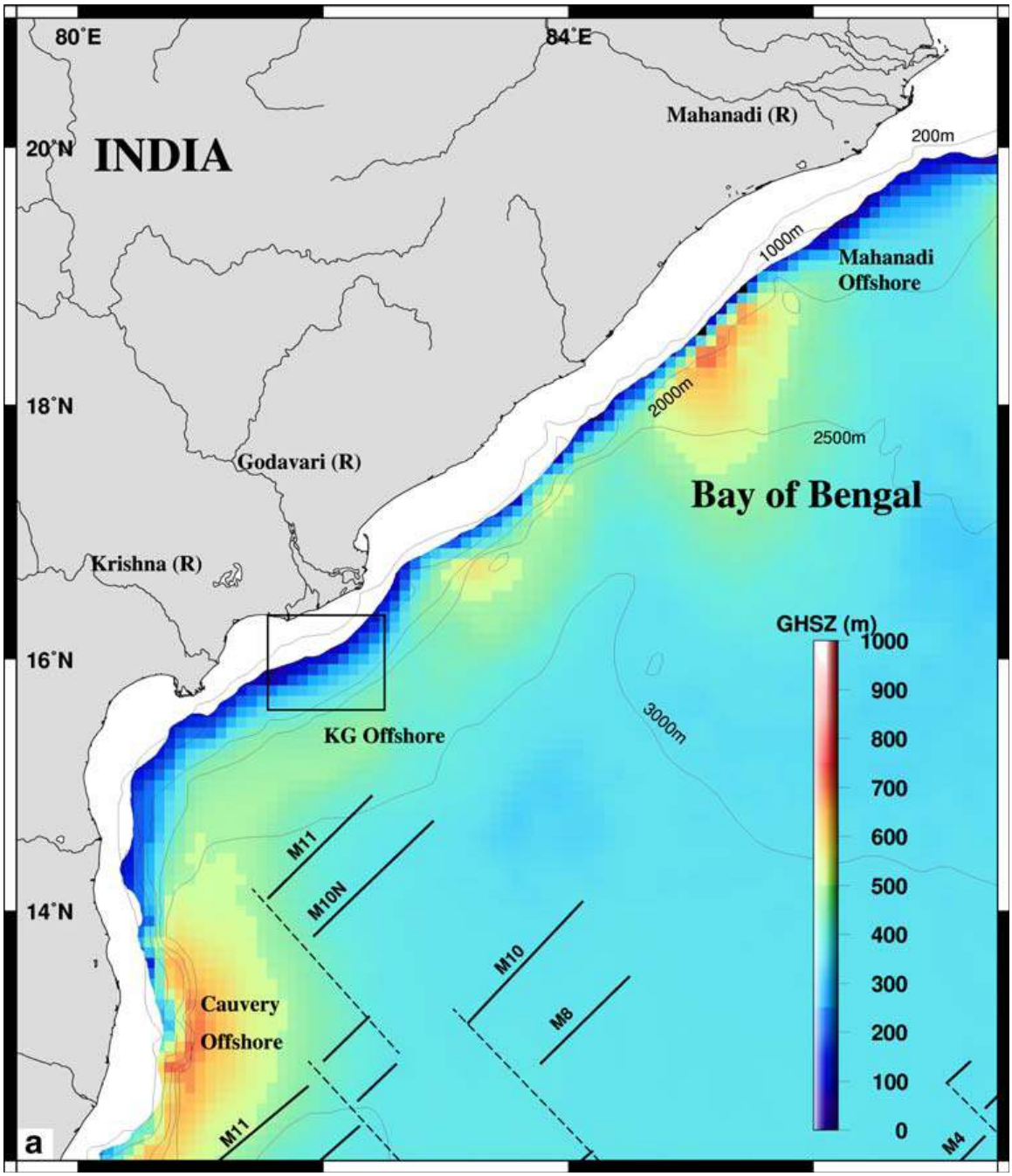
80°E
84°E
20°N
INDIA
Mahanadi (R)
200m
1000m
Mahanadi
Offshore
18°N
2000m
2500m
Godavari (R)
Bay of Bengal
Krishna (R)
16°N
GHSZ (m)
1000
900
800
700
600
500
400
300
200
100
0
KG Offshore
3000m
M11
M10N
14°N
M10
M8
Cauvery
Offshore
M11
M4
a

Fig. 1

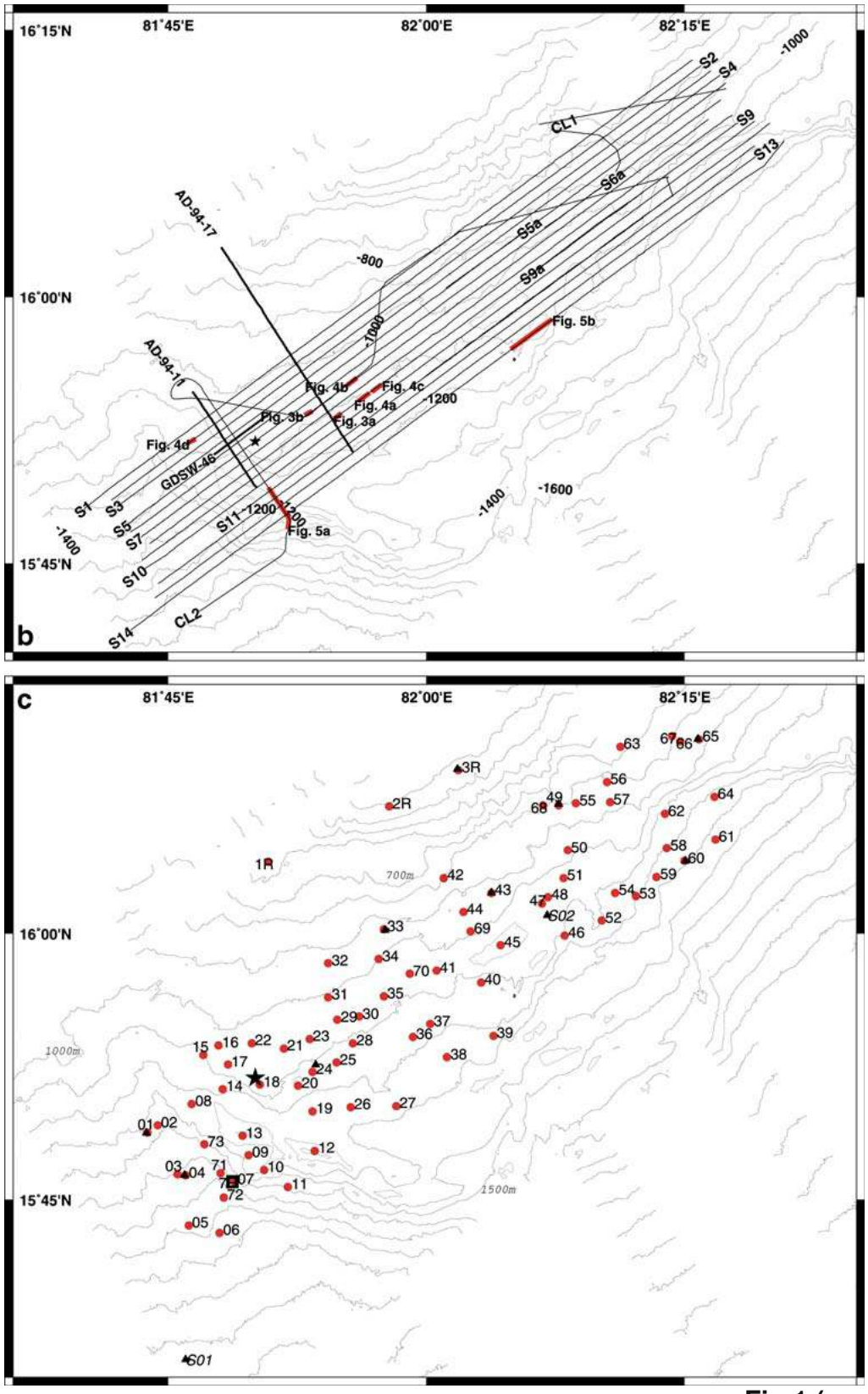

Fig.1 (continued)

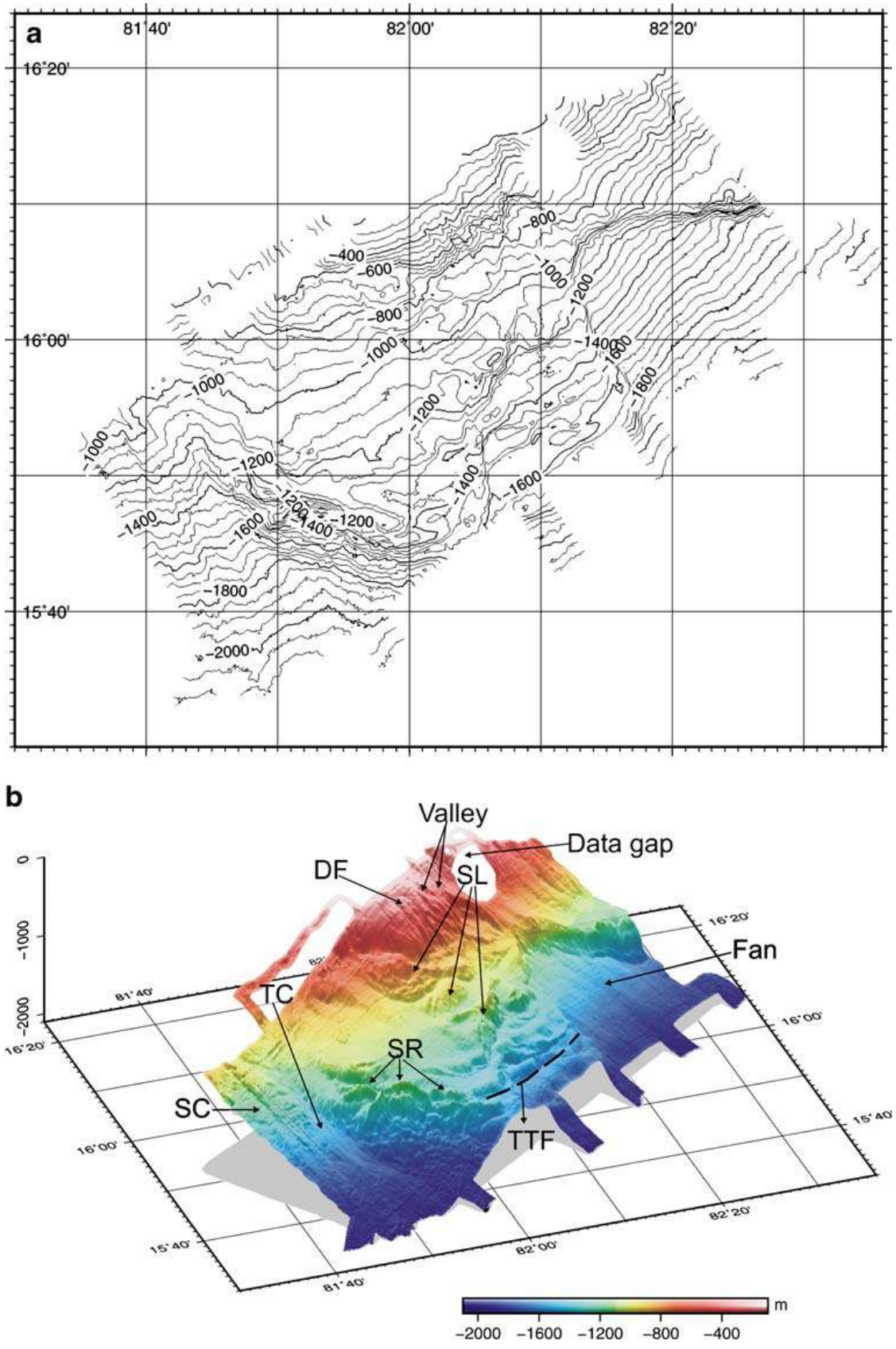
a
81°40'
82°00'
82°20'
16°20'
16°00'
15°40'
-400
-600
-800
-1000
-1200
-1400
-1600
-1800
-2000
b
Valley
Data gap
DF
SL
Fan
TC
SR
SC
TTF
0
-1000
-2000
m
-2000 -1600 -1200 -800 -400

Fig.2)

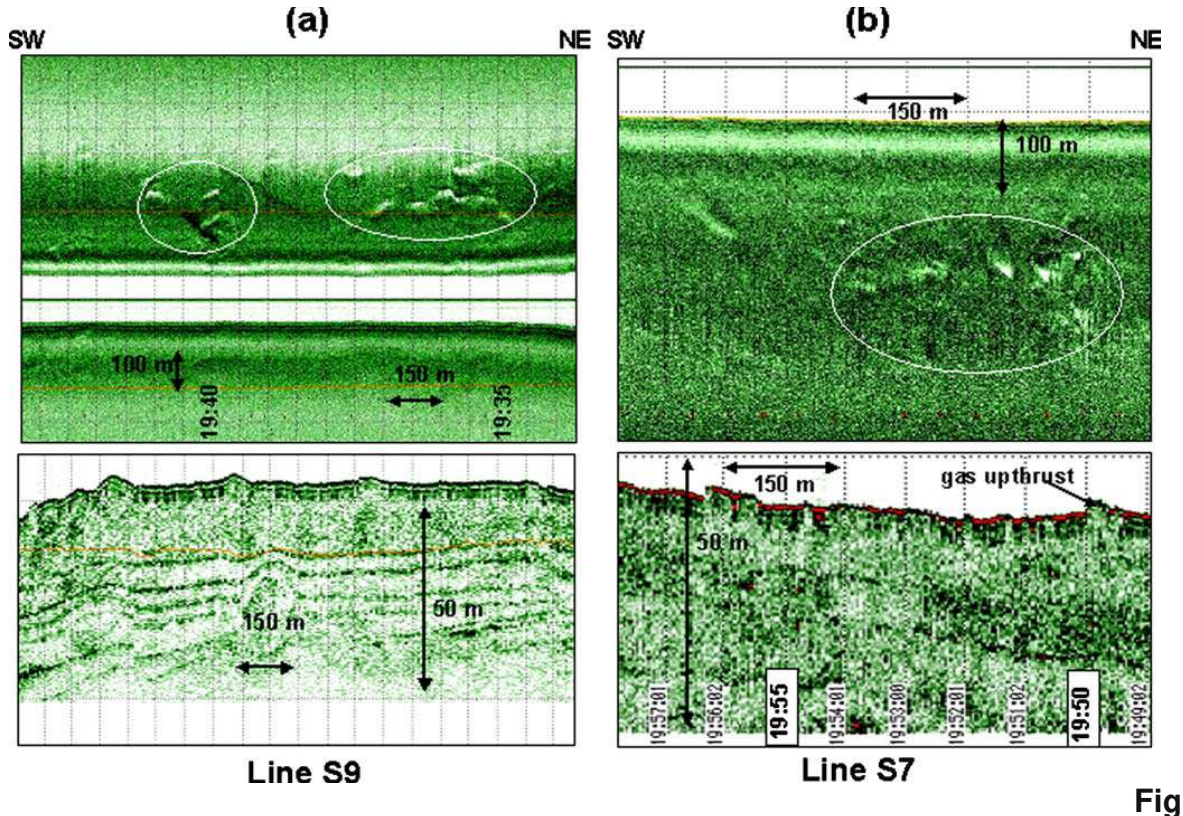

Line S9

Line S7

Fig.3

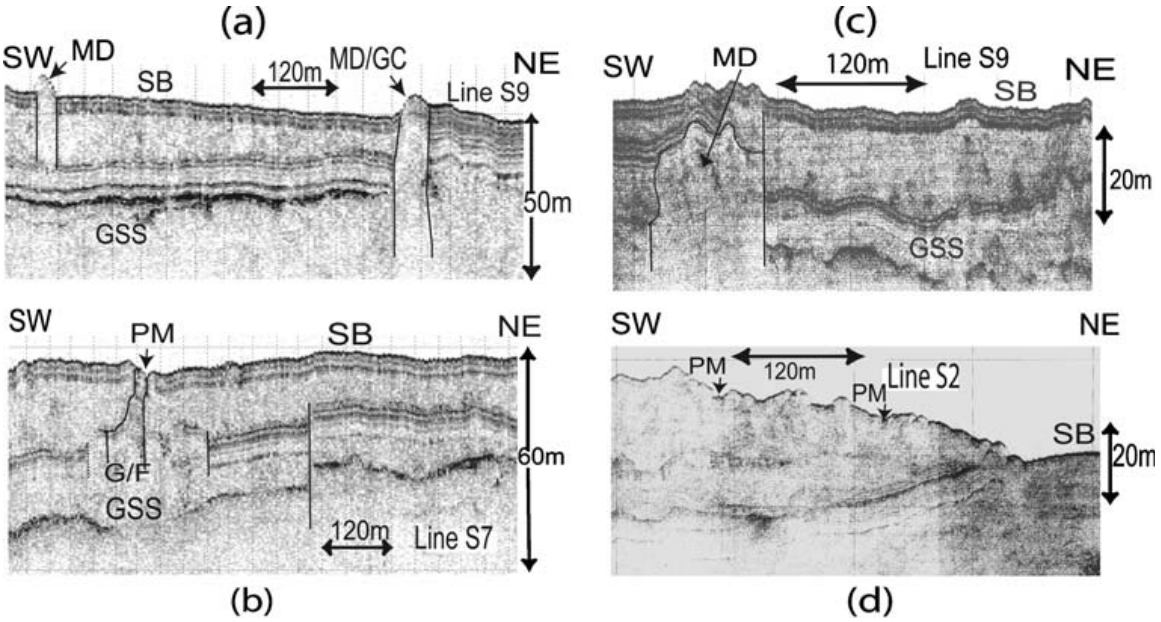
(a)
SW
MD
SB
120m
MD/GC
NE
Line S9
50m
GSS
(c)
SW
MD
120m
Line S9
SB
NE
20m
GSS
SW
PM
SB
NE
G/F
GSS
60m
120m
Line S7
(b)
SW
NE
PM
120m
PM
Line S2
SB
20m
(d)

Fig.4

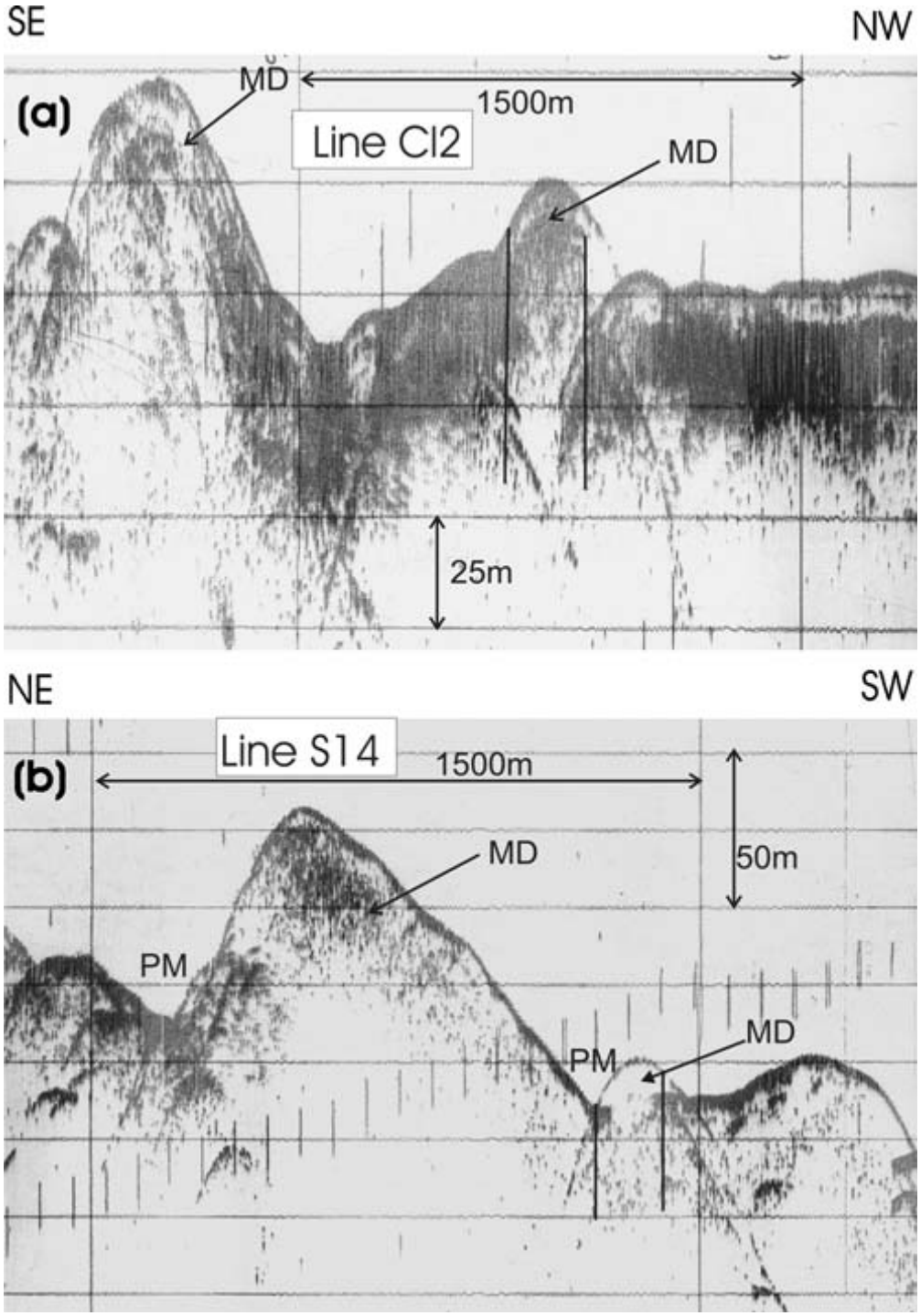
SE
NW
(a)
MD
1500m
Line CI2
MD
25m
NE
SW
(b)
Line S14
1500m
MD
50m
PM
PM
MD

Fig.5

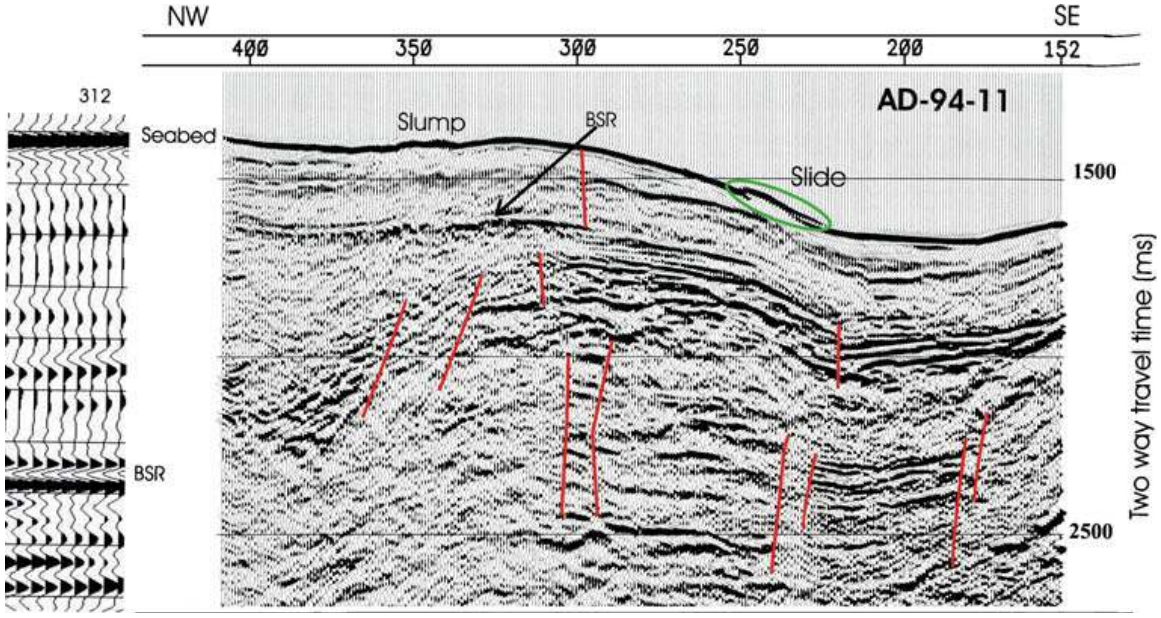
NW
SE
400
350
300
250
200
152
312
AD-94-11
Seabed
Slump
BSR
Slide
1500
2500
BSR
Two way travel time (ms)

Fig.6

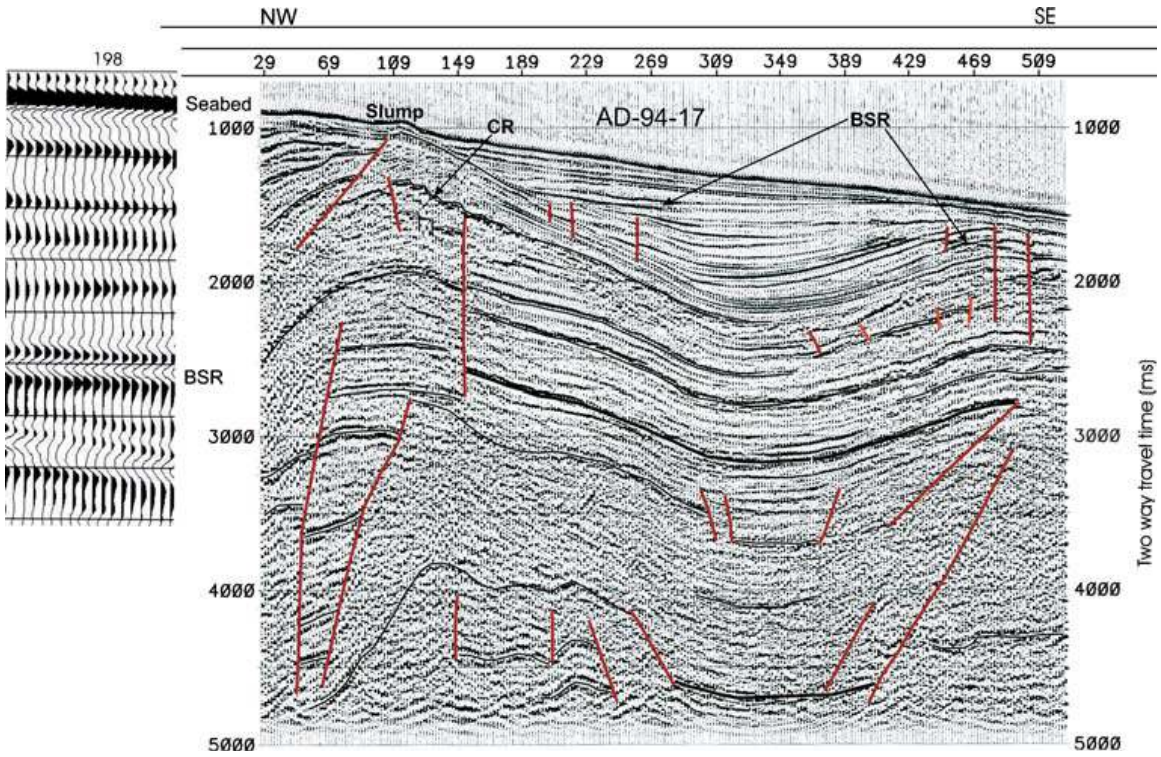
NW
SE
198
29
69
109
149
189
229
269
309
349
389
429
469
509
Seabed
1000
Slump
CR
AD-94-17
BSR
1000
2000
BSR
2000
3000
3000
4000
4000
5000
5000
Two way travel time (ms)

Fig.7

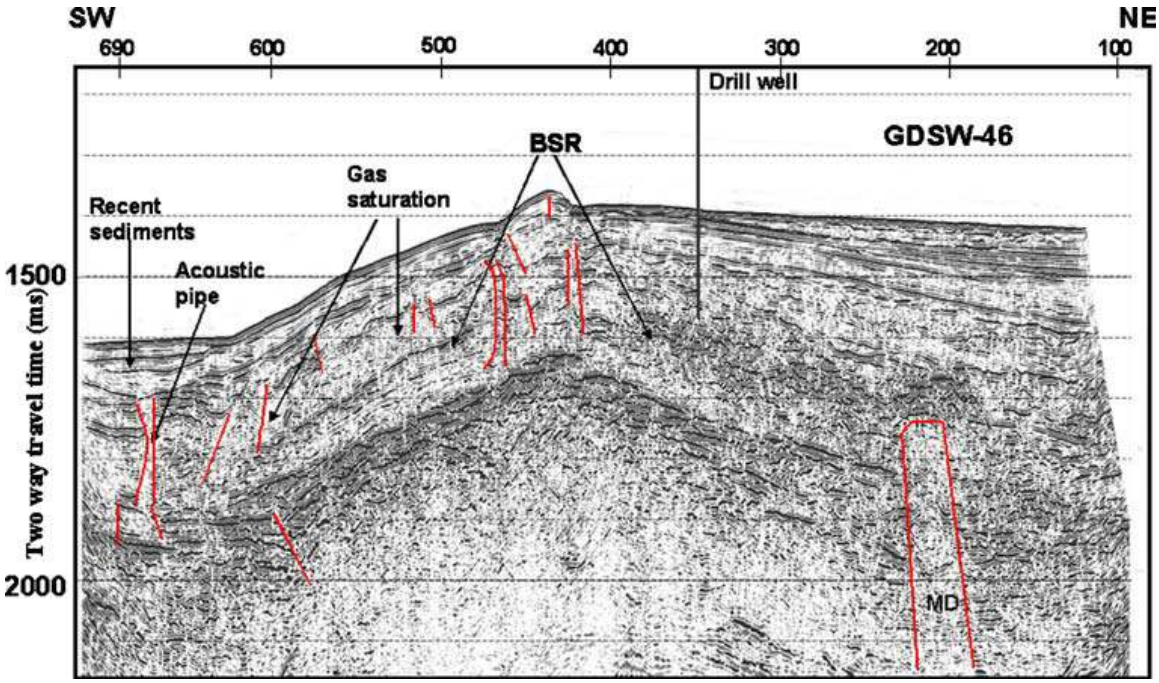
SW
NE
690
600
500
400
300
200
100
Drill well
GDSW-46
BSR
Gas
saturation
Recent
sediments
Acoustic
pipe
1500
2000
Two way travel time (ms)
MD

Fig.8

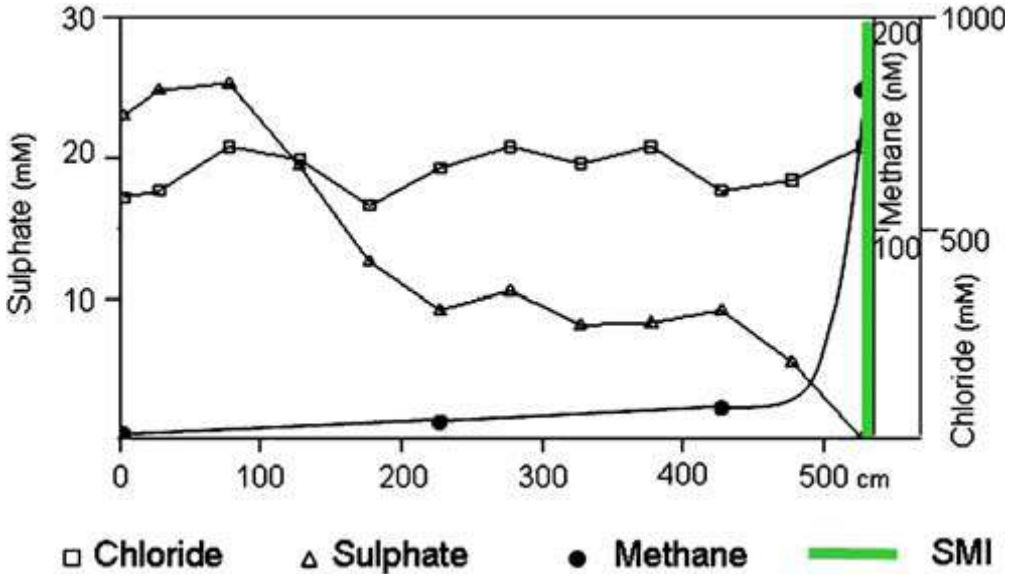
30
20
10
Sulphate (mM)
0
100
200
300
400
500 cm
200
100
Methane (nM)
1000
500
Chloride (mM)
Chloride
Sulphate
Methane
SMI

Fig.9

Fig.10